PCCP

PAPER

View Article Online
View Journal | View Issue

Cite this: *Phys. Chem. Chem. Phys.*, 2014, **16**, 14287

A DFT study on carbon monoxide adsorption onto hydroxylated α-Al_2O_3(0001) surfaces†

C. Rohmann,[a] J. B. Metson[a] and H. Idriss*[bc]

Received 29th March 2014,
Accepted 14th May 2014

DOI: 10.1039/c4cp01373e

www.rsc.org/pccp

The adsorption of CO onto the hydroxylated α-Al_2O_3(0001) surface was studied using density functional theory (DFT). Dissociated adsorption of water was found to be stable, with an adsorption energy (E_a) of 1.62 eV at θ_{water} = 0.75. The most stable hydroxylation form on the clean surface was found to be in the 1–2 dissociation configuration, where the OH group binds to a surface Al ion and the H ion binds to one of the three equivalent surface O ions. The adsorption energy of CO was found to be dependent on the degree of pre-hydroxylation of the surface as well as on the CO coverage. The highest adsorption energy of CO was found when θ_{CO} = 0.25 on a pre-hydroxylated surface with θ_{water} = 0.25; E_a = 0.57 eV. The adsorption energy of CO decreased upon increasing the degree of pre-hydroxylation. The vibrational frequency of ν_{CO} was also computed and in all cases it was blue shifted with respect to gas-phase CO. The shift, $\Delta\nu$, decreased with increasing CO coverage but increased with increasing surface hydroxylation. A comparison with available experimental work is discussed.

1. Introduction

The high temperature ceramic α-Al_2O_3 possesses good mechanical properties, is highly inert, and is used in a wide variety of technological applications.[1] Furthermore, it is applied as a substrate for thin films as well as a support for transition metals in many important classes of catalysts.[2,3] Therefore, obtaining quantitative and qualitative information on the nature of interaction with adsorbates and the effects of surface reconstructions would enhance our understanding of catalytic reactions and material properties.

The electronic structure of α-Al_2O_3(0001) has attracted experimental interest for many years.[4,5] Ahn and Rabalais[4] studying the (0001) surface, by means of time-of-flight scattering and recoiling spectrometry, atomic force microscopy (AFM) and ion trajectory simulations, reported the (1 × 1) surface to be Al-terminated. Several computational studies[6,7] also showed that the Al-terminated surface is energetically the most stable. The wide use of α-Al_2O_3 as a common support in heterogeneous catalysis has led to many studies on the adsorption of transition metals, for example, Cu,[8,9] Pd[8,10] and Pt.[11] Łodziana and Nørskov investigated the adsorption of one monolayer of Pd and Cu metals onto the stoichiometric α-Al_2O_3(0001) surface by means of density functional theory (DFT) using the GGA-PW91 exchange–correlation functional, reporting similar energies (0.9–1.0 J m^{-2}) for metal atoms preferring to occupy the hcp sites over the surface oxygen atoms. The adsorption of metals results in relatively large surface relaxations, where the topmost surface aluminium ions move towards the metals. In the presence of surface hydroxyls, Pd and Cu exhibit a weak binding to the surface.[8] However, XPS studies investigating the adsorption of Cu onto the hydroxylated (0001) surface, report an enhanced binding of Cu to the surface due to the presence of surface hydroxyls.[12,13]

There have been several studies involving the adsorption of small molecules onto the α-Al_2O_3(0001) surface. Investigations conducted on HCl[14,15] reported dissociative adsorption to be favoured. As in the case of transition metals, considerable surface relaxation is seen. Another molecule of interest is phenol[16] which was computed, using the semi-local density functional theory. The adsorption of phenol results in a binding separation (distance between the surface Al atom and the O of the phenol molecule) of 1.95 Å and an adsorption energy of 1.00 eV, with the energy increasing to around 1.2 eV when the contribution from van der Waals interactions is accounted for. Sorescu *et al.* investigating the adsorption of nitromethane onto the (0001) surface of α-Al_2O_3[17] reported the most stable configuration to occur when the molecule lays parallel to the surface and bonding with one O atom of the nitro group to the surface Al atom. Moreover adsorption in a parallel configuration was found to be 0.3 eV more stable compared to its vertical counterparts. The authors suggest that the increase in binding energy may be attributed to the repositioning of two H atoms of the methyl group which are pointing directly to the surface O atoms.[17]

[a] *School of Chemical Sciences, The University of Auckland, Auckland, New Zealand*
[b] *Department of Chemistry, The University of Aberdeen, Aberdeen, UK. E-mail: h.idriss@abdn.ac.uk*
[c] *SABIC CRI at KAUST, Thawal, Saudi Arabia. E-mail: idrissh@sabic.com*

† Electronic supplementary information (ESI) available. See DOI: 10.1039/c4cp01373e

Another molecule of great importance is water, which is present in molecular or dissociated form in the overwhelming amount of work conducted on metal oxide surfaces. In the case of corundum H ions were found to be present at temperatures as high as 1100 °C.[4] Moreover it was found that the clean, H free, Al terminated (0001) surface of Al_2O_3 readily reacts with water to form surface hydroxyls.[18–23] Water is found to be strongly and dissociatively adsorbed, with energies close to 30 kcal mol^{-1} (*ca.* 1.3 eV) depending on the local binding sites.[22] A 1–2 dissociated state in which H^+ of H_2O binds to O_S (s: for surface), the nearest neighbour surface O of Al to which the OH^- of the same H_2O binds is found to be the most stable. This was followed by a 1–4 dissociated state in which the surface O_S is across a 6-fold ring from this Al. Adsorption is accompanied by a strong relaxation of the surface. Thomas and Richardson showed that over a hydroxylated thin film surface, water does not totally wet the surface as less than 50% of the surface is covered even at exposure equivalent to 7 monolayers.[24]

A DFT study has considered a set of water adsorption and dissociation intermediates along the path from the dry to the fully hydroxylated surface.[23] A molecular water layer was found to saturate at $2H_2O/Al_s$, with half the water bound through O to Al_s and the other half bound through H to O_S, forming a hexagonal, hydrogen-bonded water ''bilayer'' above the alumina plane. These molecular water states were found to be metastable. Water is reported to dissociate with its OH fragment atop Al_s and the H fragment atop O_s. The dissociation of molecularly adsorbed water to the favoured 1–2 chemisorbed state was computed by means of the climbing image nudge elastic band (CI-NEB) method to determine the minimum energy path and the transition state, and found to have a modest activation barrier of 0.19 eV.[23]

CO is among the most commonly investigated probe molecule revealing fundamental information, such as the surface structure, adsorbate–surface interaction, adsorption behaviour and coverage dependent CO vibrational shifts, on a variety of metals, semiconductors and insulators. Computationally, it has been studied on many oxide systems, including α-Al_2O_3(0001),[25,26] Cu_2O(111),[27] MgO,[28] CeO_2,[29] and TiO_2.[30,31] In addition, it has been experimentally studied on a considerable number of metal oxides mainly by vibrational spectroscopic methods.[32–36] CO adsorption onto transition metals such as Pt[37] causes a weakening of the CO bond, which in turn results in shifting the frequency of the CO bond to lower wavenumbers (red shifted) with respect to that of gas-phase CO. Its adsorption onto metal oxides without d electrons in the valence band such as TiO_2[32] strengthens the CO bond. Upon increasing the coverage significant changes in the vibrational frequency of adsorbed CO have been reported, for example, the adsorption onto ZnO,[38] α- and γ-Al_2O_3,[26,39,40] TiO_2,[34] and Pt(111).[37]

The adsorption of CO onto Al_2O_3 was computationally studied using an Al_8O_{12} cluster model.[25] The configuration with the bond through the C moiety of CO and the Al surface is the most stable. The bond is mainly due to σ donation to the $3p_z$ and $3d_z^2$ orbitals from the CO adsorbate to the Al surface. The adsorption energy was found to be close to 0.6 eV, while the vibrational frequency of adsorbed CO (ν CO mode) was blue shifted with respect to the gas-phase molecule (44 cm^{-1}). In our previous study,[26] studying the coverage dependent adsorption of CO onto the (0001) surface of α-Al_2O_3, a blue shift, with respect to gas phase CO, of 56 cm^{-1} and 30 cm^{-1} was observed for the lowest and highest coverage investigated, respectively. Experimental infrared (IR) studies on CO interaction with α-Al_2O_3 powder[33,41] indicated a blue shift of 20 to 40 cm^{-1} with respect to gas phase CO.

In this work we present a study of the adsorption of CO onto the hydroxylated (0001) surface of α-Al_2O_3. In particular, we focus on the surface relaxation, the electronic structure upon CO adsorption and the change in the vibrational frequency of CO with respect to different surface coverage of CO and water.

2. Computational details

The calculations were conducted using the plane-wave DFT calculations as implemented in the CASTEP (Cambridge Serial Total Energy Package) simulation package.[42] Electron exchange and correlation are described using the Perdew–Burke–Ernzerhof (PBE)[43] functional of the generalized gradient approximation (GGA). For the *k*-point sampling of the Brillouin zone, Monkhorst–Pack grids[44] were used. Ultrasoft pseudopotentials[45] were employed to lower the required basis set size. A cut-off of 400 eV was used for the bulk, (1 × 1), and (2 × 2) surfaces of α-Al_2O_3. A (5 × 5 × 2) set of *k*-points for the bulk and a (3 × 3 × 1) set for the surface calculations were used, while (6 × 6 × 1) for the (1 × 1) surface. To account for the insulating behaviour of Al_2O_3, the electronic occupation numbers were fixed during minimization. Atomic positions were optimized using the BFGS algorithm[46] with an energy convergence criterion of 5.0 × 10^{-6} eV $atom^{-1}$, a force convergence criterion of 0.01 eV $Å^{-1}$ and a displacement convergence criterion of 5 × 10^{-4} Å applied.

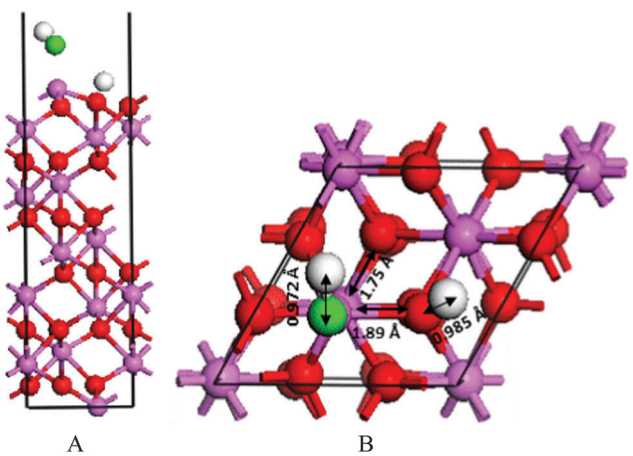

Fig. 1 (A) 1–2 water dissociation representing the full coverage on the (1 × 1) surface of α-Al_2O_3(0001) in side view and (B) top view. Al and O atoms are in purple and red, respectively, while H and O atoms of H_2O are in light grey and green, respectively.

The crystal structure of α-Al_2O_3 can be described as a rhombohedral unit cell containing two formula units of Al_2O_3 with lattice parameters a = 5.128 Å and α = 55.29°. This corundum structure can also be described as a hexagonal cell, containing six formula units of Al_2O_3 having the lattice parameters a = 4.760 Å and c = 12.989Å.

To validate our computational parameters, the optimized bulk lattice parameters, the bulk modulus, and the cohesive energy of α-Al_2O_3 have been computed. All values obtained were in good agreement with the previous experimental and computational studies conducted on α-Al_2O_3.[14,26,47,48] A detailed listing and comparison of these values can be found in our previous investigation regarding the coverage dependent CO adsorption onto the clean α-Al_2O_3(0001) surface.[26]

Table 1 Comparison of layer relaxation of the fully hydroxylated (1 × 1) surface along the z-axis in % and Å with respect to the unrelaxed structure

	Clean surface (%)	Clean surface (Å)	Hydroxylated surface (%)	Hydroxylated surface (Å)
Al_1/O_2	−89.98	−0.760	−14.64 (−13)[a]	−0.124 (−0.11)[a]
O_2/Al_3	+3.19	+0.027	−0.72	−0.006
Al_3/Al_4	−45.11	−0.225	−31.98	−0.160
Al_4/O_5	+20.16	+0.170	+10.34	+0.087
O_5/Al_6	+6.23	+0.053	+0.43	+0.004

Negative signs indicate the movement of two layers towards each other, while the positive ones indicate that apart from each other. The subscript number indicates the layer number starting from the surface. [a] From ref. 22.

In order to compute for the vibrational frequency of CO adsorbing onto the hydroxylated Al_2O_3(0001) surface, Dunham analysis was employed.[49] While simulating the CO/OH vibration, by changing the C–O/O–H bond distance in steps of 0.02 Å, the centre of weight was kept throughout the entire process. The presented results were obtained using a quartic fit of 7 points.

3. Results and discussion

3.1 Free H_2O and CO

The calculations of gas-phase CO and H_2O at the gamma point were performed by placing the molecule in a cubic cell of 10 Å. In the case of water an O–H bond length of 0.977 Å and an H–O–H angle of 104.48° were obtained. Both values are in good agreement with those found by experimental[50] and computational[51] investigations. The free CO molecule revealed a bond length of 1.154 Å also in agreement with previous studies[25] and a C–O stretching vibration of 2170 cm^{-1} which is shifted by 27 cm^{-1} with respect to the experimental value of 2143cm^{-1}. In a 10 × 10 × 10 $Å^3$ cell the energy of the free H_2O molecule is equal to −468.77 eV while that of the free CO molecule is −590.16 eV.

3.2. α-Al_2O_3(0001) surface

Following our previous work,[26] the (0001) surface is described by an 18 layer thick slab (six stoichiometric layers) where the top 11-layers were allowed to relax while the seven bottom

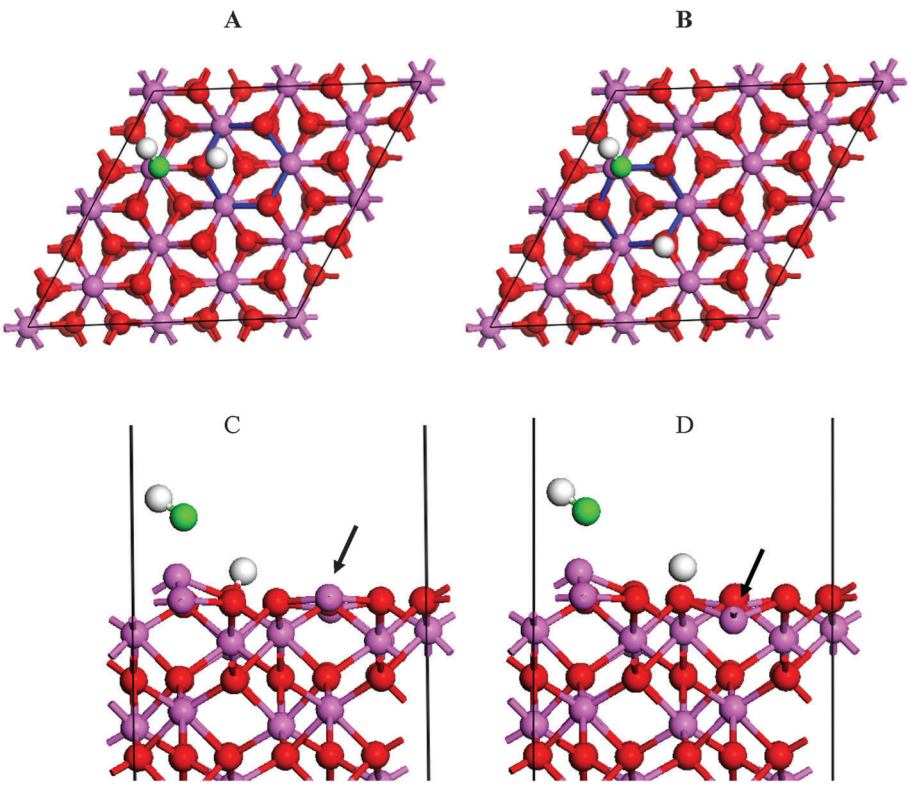

Fig. 2 The (2 × 2) Al_2O_3(0001) surface representing (A) the 1–2 and (B) 1–4 dissociation of water. (A) and (B) Top views showing the H to adsorb in 1–2 configuration onto one of the nearest neighbour O atoms, while the H in 1–4 configuration adsorbs across a six-fold ring (blue) with respect to the Al adsorption site. (C) and (D) Side views of the 1–2 and 1–4 dissociation of water.

layers were frozen at the bulk geometry, a 14 Å vacuum layer was added.

Consistent with other studies,[8,47,52,53] the optimised clean surface reveals a strong inward relaxation of the top Al layer into the following O layer, resulting in a decrease in the Al–O bond length. This strong inward relaxation, caused by charge redistribution from Al to O[7], is responsible for the large difference in surface energy between the relaxed and unrelaxed structures, 1.54 J m^{-2} and 3.50 J m^{-2}, respectively.

By comparing the density of states (DOS) of the bulk and the relaxed surface, splitting of the bands in the 7 to 12 eV region is seen in addition to a decrease of the band gap by *ca.* 2 eV.[26]

3.3. CO adsorption onto the (0001) surface

The adsorption of CO onto the (0001) surface of α-Al_2O_3 was previously studied, the main observations are summarised in the following.

The most stable CO adsorption is found at the lowest coverage investigated, 25%. The vibrational frequency of ν CO revealed a coverage dependent blue shift with respect to gas phase CO in line with the experimental work conducted on ZnO[38] and TiO_2 powder.[34] All examined adsorbate coverage revealed a partial relief of the strong relaxation on the Al adsorption site interacting with a CO molecule, this relief was found to increase with decreasing CO coverage. The change in the adsorption energy of CO on the surface is best explained as due to changes in the surface structure and not due to lateral CO interactions. A summary of the structural and vibrational changes upon different CO coverage is provided in Table SM1 (ESI†).

3.4. The hydroxylated (0001) surface of α-Al_2O_3

As mentioned in the Introduction section, the Al terminated (0001) surface of Al_2O_3 readily reacts with water to form surface hydroxyls.[18–23]

The dissociated H_2O molecule was placed in the 1–2 configuration, the OH group on top of the Al adsorption site and the H on top of one of the nearest neighbour O (Fig. 1). The (2 × 2) and (1 × 2) surfaces were employed to study the water coverage of 25%, 50%, 75% and 100%.

In good agreement with previous studies with respect to surface geometry and adsorption energy,[22,23] we found that water adsorption onto the (1 × 1) surface (100% coverage) is stable in the 1–2 configuration, exhibiting an adsorption energy of 1.45 eV. Table 1 presents the changes in the interlayer distance upon adsorption of the OH group onto the surface Al atom. The OH group binding to the top of the surface Al layer relieves the strong surface relaxation of the Al atom into the following O layer. The surface O_S binding to the H^+ of H_2O relaxes upward compared to the remaining two O, "s" denotes a surface site. In addition, a significant change in the surface geometry occurs. The Al–O bonds with a length of 1.70 Å for the clean relaxed surface increased to 1.75 Å upon hydroxylation. The Al–O_SH bond length was found to be 1.89 Å, the O–H and

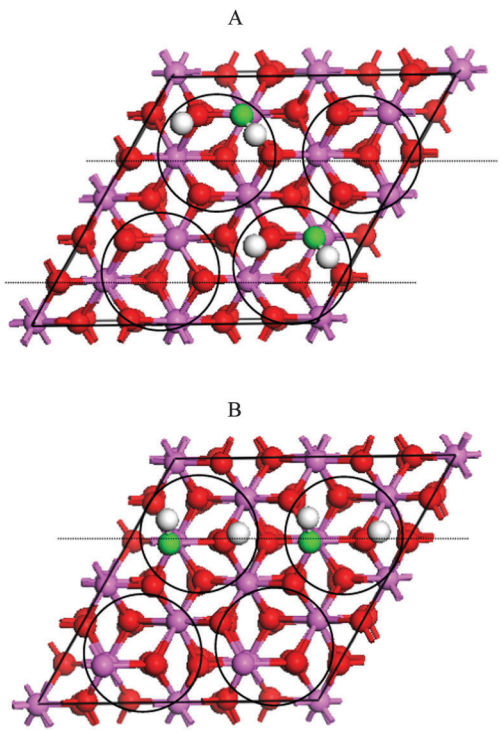

Fig. 3 A top view of dissociative water adsorption at a coverage of 50% onto the (2 × 2) Al_2O_3(0001) surface in parallel (A) and linear (B) configurations. The circles are guide to see the available pairs for the dissociative adsorption. In each surface there are four circles for the four possible water dissociative adsorptions.

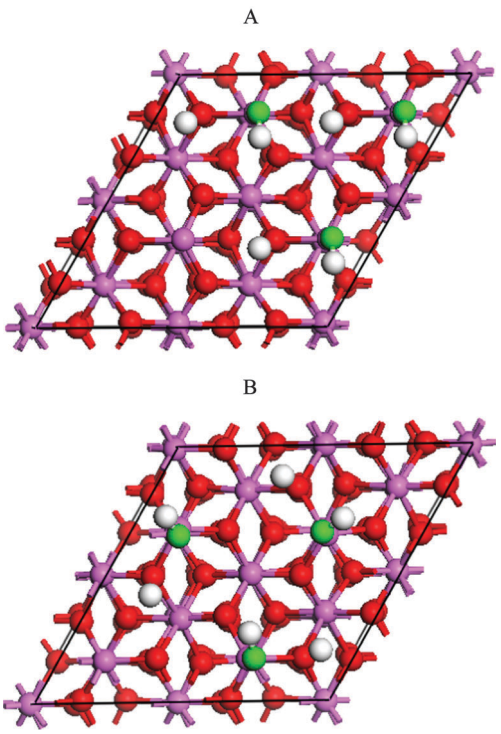

Fig. 4 A top view of two (2 × 2) surfaces exhibiting a 75% surface hydroxylation. (A) The dissociative adsorption of water inflicting the 1–4 configuration on two out of three Al adsorption sites is presented on top. (B) The dissociative adsorption of water in an arrangement where none of the occupied adsorption sites is in the 1–4 configuration.

O_S–H bonds were 0.972 Å and 0.985 Å, respectively. The OH group is tilted away from the surface normal by 59°, and the H of the O_S–H group is oriented toward one of the surface O atoms. A similar tilting behaviour has been observed in the case of methanol[54] and phenol[16] adsorption onto the (0001) surface of α-Al_2O_3.

The vibrational frequencies of the two distinct O–H stretching modes are computed to be 3917 cm^{-1} for the OH on top of the Al adsorption site and 3679 cm^{-1} for the O_SH vibrations. The difference in wavenumbers of 238 cm^{-1} is in good agreement to that of 225 cm^{-1} reported by Ranea *et al.*[23]

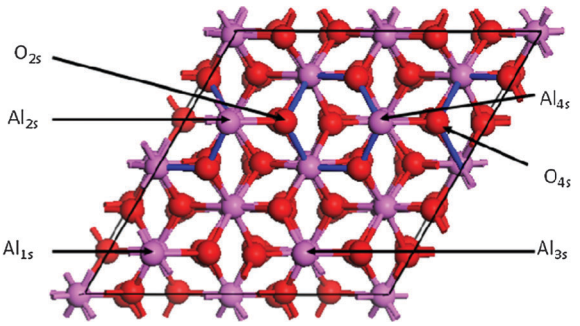

Fig. 5 The (2 × 2) α-Al_2O_3(0001) surface. The four Al adsorption sites and the 6-fold rings (blue) of the Al_{2S} and Al_{4S} adsorption sites are shown. The O_{2S} and O_{4S} adsorption sites are shown to represent 1–2 configuration/1–4 configuration with respect to the Al_{2s}/Al_{4s} adsorption sites. The subscript numbers of the O adsorption sites indicate the nearest neighbour Al adsorption site.

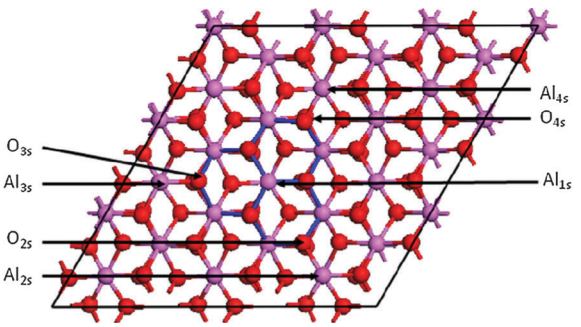

Fig. 6 A (3 × 3) surface of bare α-Al_2O_3(0001). The four Al adsorption sites and three O adsorption sites inflicting 1–4 arrangement onto the Al_{1S} site by being placed across a 6-fold (blue) are shown.

Compared to the 1–2 dissociation, the 1–4 dissociation of water (a representation of both is presented in Fig. 2) was found to be less stable, in agreement with previous reports.[22,23] The computed adsorption energies are 1.27 eV and 1.53 eV for the 1–4 and 1–2 dissociation of water at 50% coverage, respectively. Furthermore, we note the previously reported[22] large inward relaxation of the free Al adsorption site bound to the O_SH in the 1–4 configuration, which can also be seen in Fig. 2D. A less pronounced but similar behaviour is seen in the case of the 1–2 dissociation. In the following, we will refer to all adsorption sites in a 1–4 environment to be in the 1–4 configuration.

Experimental studies conducted on α-Al_2O_3(0001) single crystals by means of Fourier transform infrared spectroscopy (FTIR)[24,55] and sum-frequency vibrational spectroscopy (SFVS)[56] showed the existence of surface hydroxyls as well as of ordered molecularly adsorbed water.[55] The SFVS measurements identified two main features at 3700 cm^{-1} and 3430 cm^{-1}. These peaks are attributed to OH species based on isotope-substitution experiments. The strong peak at 3700 cm^{-1} assigned to O_S–H vibrations is close to the computed value of 3679 cm^{-1} in this study. The feature observed at 3430 cm^{-1}, not observed in this work, was assigned to bonded OH stretching of adsorbed water molecules.[24,55]

To further investigate the effect of dissociatively adsorbed water, the coverage of 25%, 50%, 75% and 100% was analysed with respect to surface relaxation and vibrational modes. We will limit our focus of the 50% and 75% coverage to two cases exhibiting different structural arrangements (Fig. 3 and 4). In the case of 50% coverage, the 1–2 dissociation of water is investigated with respect to the 1–4 configuration of the free adsorption site (*parallel arrangement*) and the OH occupied Al adsorption site (*linear arrangement*) (Fig. 3). A linear arrangement of two dissociated water molecules causes both adsorption sites to inflict a 1–4 configuration upon each other (Fig. 3). This assumes that the initial 1–2 dissociation of water takes place at the Al_{2S} and O_{2S} adsorption sites, Fig. 5. The OH and H of the second dissociated water molecule are on top of the Al_{4S} and O_{4S} sites, respectively. Therefore, one finds the Al_{4S} site in 1–4 configuration with respect to the O_{2S} site as it finds itself across a 6-fold ring (blue). Also, the Al_{2S} site is in 1–4 configuration with respect to the O_{4S} site. In the case of a parallel arrangement only the empty Al adsorption site is in 1–4 configuration.

In the case of surface hydroxylation of 75% two models were considered. The first adopting the 1–4 configuration (*linear*) with respect to the occupied Al adsorption sites of the 50%

Table 2 Structural and vibrational properties of adsorbed H_2O onto α-Al_2O_3(0001). Values italicized present water adsorption onto an Al adsorption site in 1–4 configuration

Surface	(2 × 2)	(2 × 2)	*(1 × 2)*	(2 × 2)	*(2 × 2)*	(1 × 1)
Coverage [%]	25	50	*50*	75	*75*	100
$r_{Al–OH}$ [Å]	1.725	1.721[a]	*1.723*	1.716[a]	*1.718*[a]	1.720
$r_{Os–H}$ [Å]	0.971	0.971[a]	*0.971*	0.971[a]	*0.971*[a]	0.972
$\nu_{Os–H}$ [cm^{-1}]	3707	3712	*3648*	3692	*3670*	3679
$\nu_{O–H}$ [cm^{-1}]	3934	3918	*3927*	3928	*3929*	3917
Adsorption energy [eV]	1.54	1.53	*1.44*	1.62	*1.47*	1.45

For comparison the adsorption energy of H_2O using un-relaxed Hartree–Fock calculation of the CRYSTAL code gave adsorption energy (binding energy) = 1.31 eV, 1.53 eV, and 1.29 eV, for the molecular, 1–2, and 1–4 configuration, respectively.[60] This is to be compared to 1.01 eV, 1.44 eV, and 1.41 eV for the three modes using CPMD with GGA/BLYP.[22] [a] An average value is presented.

coverage and adding one dissociated water molecule to the surface as presented in Fig. 4A. In the second configuration all water molecules were placed in an arrangement which avoids 1–4 configuration to any occupied Al adsorption site (Fig. 4B). This configuration causes the empty adsorption site to be in 1–4 configuration with respect to the dissociative adsorption of water. This is illustrated using a (3 × 3) super cell in Fig. 6 where H is bound to the O_S sites labelled O_{2S}, O_{3S}, and O_{4S}, therefore, causing the Al_{1S} adsorption site to be in 1–4 configuration with respect to all remaining Al adsorption sites.

Some of the changes upon the coverage-dependent adsorption of dissociated water onto α-Al_2O_3(0001) are listed in Table 2. Upon an increase in surface hydroxylation, a negligible change in the O_S–H and O–H distances is observed. While changes are seen with respect to the adsorption energy, for Al–OH bond lengths, O_S–H and O–H vibration there is no clear pattern with respect to an increase in surface hydroxylation. The most stable configuration is a coverage of 75%, inflicting a 1–4 configuration to the free adsorption site. The increase in adsorption energy compared to the 25% surface hydroxylation can be linked to structural relaxation. The lateral relaxation of the investigated surfaces was studied in detail (see ESI,† Tables SM2 and SM3 for more details). The largest upward movement of the occupied Al adsorption sites is connected to the deepest relaxation of the free adsorption site into the bulk of the surface.

Comparing these findings to our previous study of the coverage-dependent CO adsorption[26] where a linear increase in adsorption energy with decreasing coverage was noted, we found that such a trend is offset by adsorption in 1–4 configuration, creating two different adsorption environments. Plotting the adsorption energy of dissociated water *versus* coverage, the influence of the 1–4 configuration becomes evident (Fig. 7). This arrangement, of the 1–4 configuration, has a stabilising effect as shown in the case of the 75% coverage when free adsorption sites are in that configuration, while it is destabilising when inflicted upon occupied adsorption sites.

To further study the adsorbate–substrate interaction the DOS and local density of states (LDOS) plots were calculated from the (1 × 1) surface representing the fully hydroxylated surface. Fig. 8 presents the DOS of the clean and fully hydroxylated (1 × 1) surfaces as well as the free water molecules. Fig. 9 shows the LDOS plots of surface atoms at the relaxed surface with and without H_2O. The adsorption of water causes, in general, an increased population of the lower lying surface states with respect to the Al and O surface states (Fig. 9). A downshift of all occupied orbitals is seen – Table 3. The unoccupied $4a_1$ orbitals remain unchanged. The OH group on top of the surface Al can be identified by an increase in the peak formation consisting of Al 3s and 3p contribution ranging from −5.0 eV to −7.7 eV, and −1.3 eV (Fig. 9A and B). The bonding of H to O_S is seen by the formation of a peak at −8.1 eV and −20.6 eV in the LDOS representing the O_S surface states shown in Fig. 9C and D.

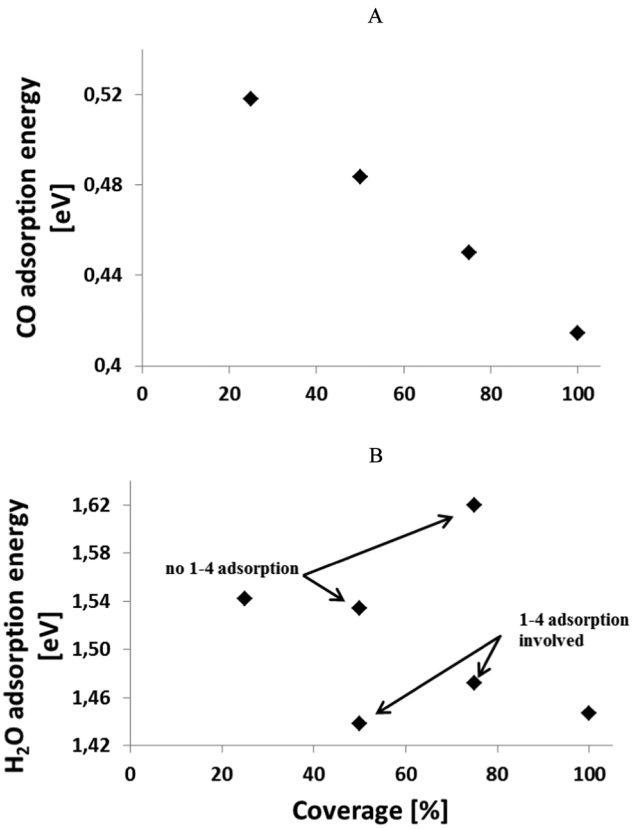

Fig. 7 (A) Coverage dependence of CO adsorption onto α-Al_2O_3(0001). (B) Coverage dependence of 1–2 dissociative water adsorption onto α-Al_2O_3(0001).

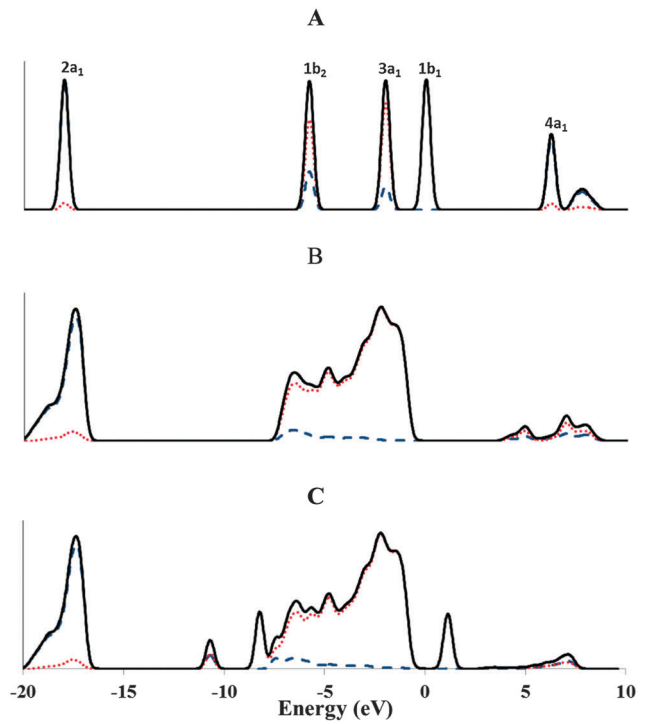

Fig. 8 (A) DOS of the free H_2O molecule. (B) LDOS (surface states only) of the clean α-Al_2O_3(0001) surface. (C) LDOS (surface states only) of H_2O adsorption onto the α-Al_2O_3(0001) surface. Dashed and dotted lines represent s and p contributions, respectively, while solid lines are the sum of s and p contributions. The Fermi level is at 0.0 eV.

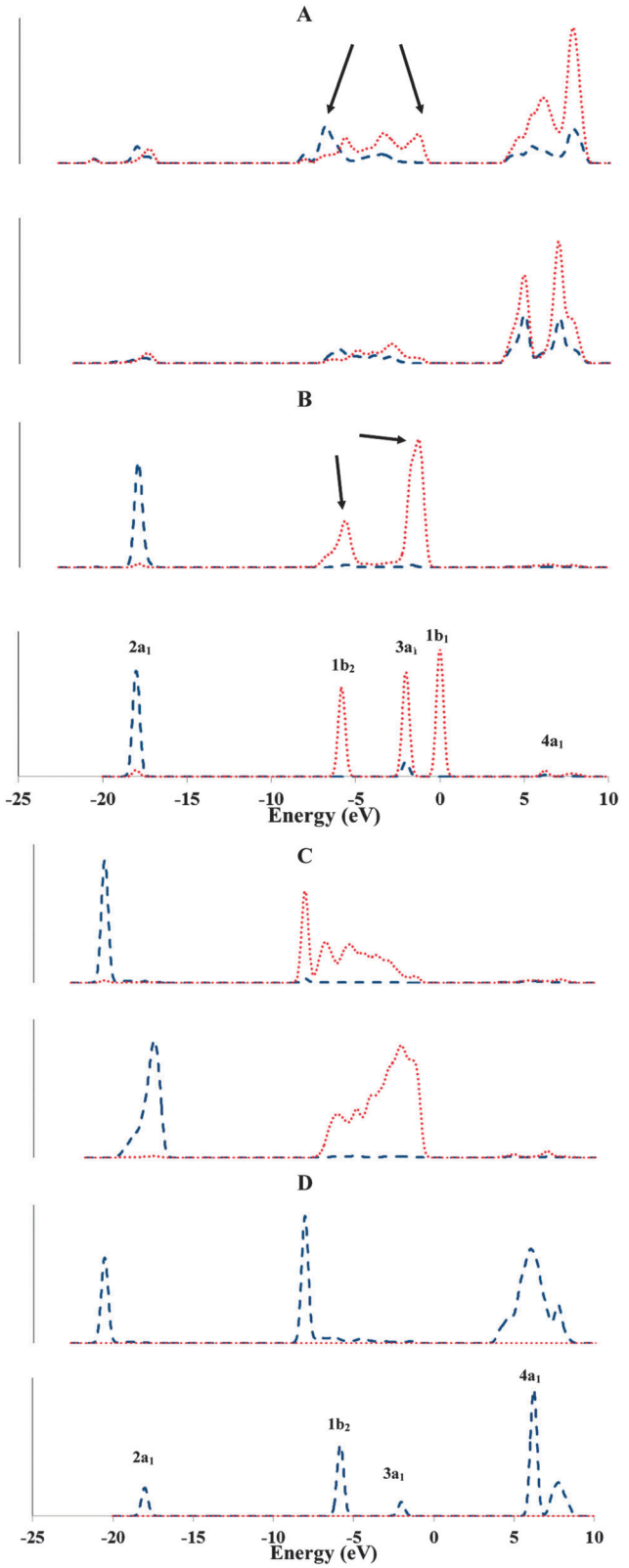

Fig. 9 (A) LDOS plots of Al surface states of H_2O/α-Al_2O_3(0001) and α-Al_2O_3(0001). (B) LDOS plots of O (O–H) surface states of H_2O/α-Al_2O_3(0001) and O of H_2O(g). (C) LDOS plots of O of O_s–H states of H_2O/α-Al_2O_3(0001) and O of α-Al_2O_3(0001). (D) LDOS plots of H of O_S–H states of H_2O/α-Al_2O_3(0001) and H of H_2O (g). Dashed and dotted lines are s and p contributions, respectively. The Fermi level is at 0.0 eV.

3.5. CO adsorption onto the hydroxylated (0001) surface of α-Al_2O_3

The CO adsorption onto the hydroxylated surface was modelled by placing the CO molecule perpendicular (with the C of CO facing the surface) on top of an Al adsorption site. The effects of two coverage-dependent adsorption behaviours were examined. In the first case, the coverage of CO molecules adsorbed onto a surface exhibiting a pre-existing water coverage of 25% was changed, whereas in the second case, the CO coverage was kept constant at 25% on surfaces exhibiting 25%, 50% and 75% hydroxylation.

The structural and vibrational properties listed in Table 4 show that the adsorption of one CO molecule onto a 25% pre-hydroxylated surface is most stable. The adsorption of CO onto an Al adsorption site in 1–4 configuration yields a much weaker binding of CO, 0.44 eV (see Table SM4, ESI†). Since this surface represents a CO coverage of 25% with one dissociated water molecule, the surface has a total coverage of 50% with respect to the Al adsorption sites. Therefore, it is worth to compare CO adsorption behaviour at a hydroxylated surface to that of the dry surfaces exhibiting 25% and 50% CO coverage (see ESI,† Table SM1 and Table 4). The CO adsorption energy of 0.57 eV on the hydroxylated surface is slightly stronger than that of 0.52 eV and 0.48 eV on the dry surface with a CO coverage of 25% and 50%, respectively. The vibrational frequency and the CO bond distance are very close to those of the dry surface representing 25% coverage, but differ significantly from those of 50% CO coverage.

Table 3 Energy level in eV for H_2O orbitals for free and adsorbed water on α-Al_2O_3(0001). Δ is the difference in eV

Orbital	Free H_2O	H_2O/α-Al_2O_3	Δ
$4a_1$	+6.2	+6.2	+0.0
$1b_1$	+0.0	−1.3	−1.3
$3a_1$	−2.0	−5.7	−3.7
$1b_2$	−5.8	−8.1	−2.3
$2a_1$	−18.0	−20.6	−2.6

Table 4 Structural and vibrational properties of an increased CO coverage to the (2 × 2) surface of α-Al_2O_3(0001) exhibiting a water coverage of 25%

	2 × 2	2 × 2	2 × 2	2 × 2	2 × 2[b]
H_2O coverage [%]	25	25	25	25	25
CO coverage [%]	0	25	50	75	75 (1–4)
Total coverage	25	50	75	100	100
r_{C-O} [Å]	—	1.148	1.149[a]	1.151[a]	1.152
r_{Al-C} [Å]	—	2.161	2.157[a]	2.177[a]	2.207
r_{Al-OH} [Å]	1.725	1.731	1.738	1.748	1.748
r_{O-H} [Å]	0.971	0.971	0.971	0.972	0.972
r_{Os-H} [Å]	0.985	0.985	0.984	0.981	0.981
ν_{C-O} [cm^{-1}]	—	2225	2223[a]	2208[a]	2201
Δ_{C-O} [cm^{-1}]	—	55	53[a]	38[a]	31
ν_{O-H} [cm^{-1}]	3934	3936	3927	3924	3924
ν_{Os-H} [cm^{-1}]	3707	3696	3696	3747	3747
CO adsorbtion energy [eV]	—	0.57	0.54	0.43	0.43

Only at 75% CO coverage, the adsorption of one CO molecule takes place in a 1–4 configuration. [a] An average value of the two equivalent CO molecules is presented. [b] The CO molecule finding itself in the 1–4 configuration with respect to the protonated surface O_S.

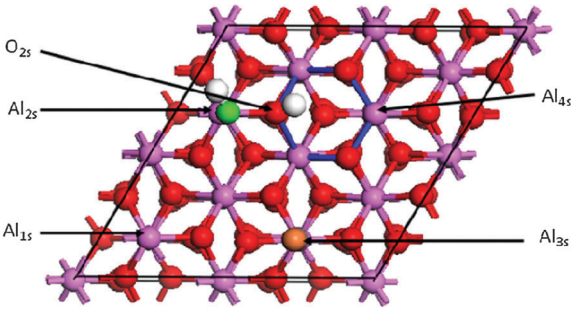

Fig. 10 The (2 × 2) surface showing 1–2 dissociation of water at the Al_{2S} and O_{2S} sites, whereas CO adsorption takes place at the Al_{3S} site. For clarity, the O atom of CO is in orange. The empty adsorption Al_{4S} site is located across a 6-membered ring, therefore being in 1–4 configuration.

3.5.1. Increasing the CO coverage on the hydroxylated surface. The coverage-dependent adsorption of CO was investigated using a (2 × 2) surface preoccupied by one dissociated water molecule, thus leaving the Al_{4S} site in 1–4 configuration, with respect to Fig. 10. The increase in CO coverage is modelled by occupying subsequently the Al adsorption sites Al_{3S}, Al_{1S}, and Al_{4S}, as shown in Fig. 10.

An increase in the CO bond length ranging from 1.148 Å to 1.152 Å is noted, still lower than that of 1.154 Å for the free CO molecule. Associated with the increase in the CO bond length is a decrease in CO wavenumbers from 2225 cm^{-1} to 2201 cm^{-1} and a decrease in the CO binding energy from 0.57 eV to 0.43 eV. The O–H bond length remains unaffected, although a decrease in the OH vibrations from 3936 cm^{-1} to 3924 cm^{-1} with the increase of the CO coverage is seen. At a CO coverage of 75%, significant structural changes are observed. These changes are very likely to result from the 1–4 configuration of the free Al_{4S} adsorption site where the final CO molecule was added. The most notable change is the decrease in the interlayer distance of the Al_{2S} site bound to the OH fragment from 0.748 Å to 0.706 Å upon an increase in CO coverage. This is accompanied by a steady relaxation of the O_S site binding to the H into the top O layer. CO adsorption onto Al_{3S} also shows a trend of decreasing interlayer distances upon an increase in CO adsorption. A similar relaxation pattern was noted for the coverage-dependent CO adsorption onto the dry surface. Comparing the results of a surface with a hydroxylation of 25% in the presence of one CO molecule to a 25% surface hydroxylation in the absence of CO, we note the following three observations: (1) An enhanced relaxation with respect to the relaxation of the Al_{2S} site. (2) A further inward movement of the Al_{4S} site into the bulk. (3) The O_S site binding to the H reveals a slightly shorter interlayer distance to the following O layer.

3.5.2. Effect of degree of hydroxylation on CO adsorption. CO adsorption onto an increasingly hydroxylated surface (25%, 50% and 75%) is presented in Fig. 11 and Fig. SM2, ESI.† The cases investigated represent the most stable hydroxylated surfaces, with the exception of the 75% surface hydroxylation. In this case, both previously examined surface arrangements were being considered, see Fig. 4. The adsorption of CO was found to be stable for all investigated coverage with the exception of the 75% surface hydroxylation, as presented in Fig. 4B. Since the free Al adsorption finds itself far below the surface plane, no CO adsorption is plausible.

Tables 5–7 present the structural and vibrational properties of CO and water with increasing hydroxylation. With the exception of the Al–C bond length increasing from 2.161 Å to

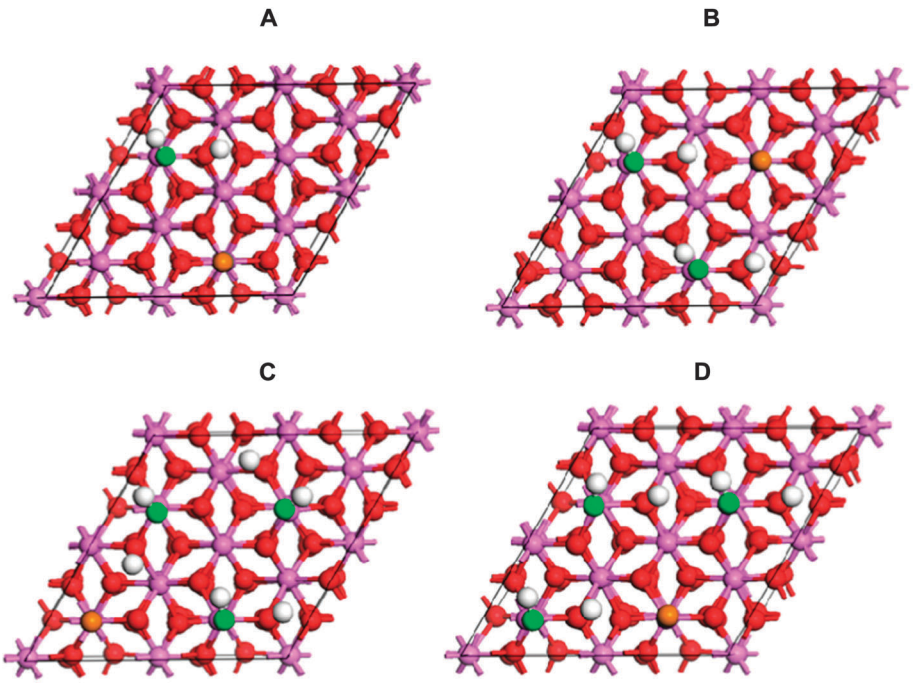

Fig. 11 (a) 25% hydroxylation, 1–4 inflicted on the free Al adsorption site. (b) 50% hydroxylation, 1–4 inflicted on CO and the free adsorption site. (c) 75% hydroxylation, structure A. (d) 75% hydroxylation, structure B. All results are on the 25% CO coverage.

2.177 Å, the remaining C–O, Al–OH, O–H and O_S–H bond distances are little affected. The O_S–H vibration belonging to the Al–OH site inflicting 1–4 configuration upon the CO adsorption site (which is the free Al adsorption site in Fig. 4A) shifted to higher wavenumbers compared to their counter part acting in the same way on a free or OH occupied Al adsorption site. Also an increase in the CO vibrational frequency to approximately 2240 cm^{-1} upon surface hydroxylation at and above 50% is noted, while the CO adsorption energy was found to decrease with increasing surface hydroxylation.

It is clear from this work that the main effect on the adsorption energy of CO on the α-Al_2O_3(0001) surface is structural variations and not electronic. This is in large due to the initial strong relaxation of the last atomic layer, whereby the Al atoms relax downwards from the bulk position due to strong electrostatic bonds with oxygen atoms. The adsorption of CO or water partially reverts this process locally. Thus any adsorption adjacent to this is largely affected by surface reconstruction. Unlike the case of TiO_2, for example[57] (where the lateral effect takes place), these large reconstructions allow for a restricted local environment where the second adsorption takes place, as seen for example in Fig. 2 and Tables 5 and 6 where the 1,2 configuration allows for a stronger bonding when compared to the 1,4 configuration. One of the implications of these observations may be considered in the case of the adsorption of CO onto the M/α-Al_2O_3(0001) surface. Because of the weak interaction of CO with the α-Al_2O_3(0001) surface and the absence of the lateral attractive effect CO would preferentially bind to the metal at low coverage. In a work focusing on the adsorption of CO onto α-Al_2O_3(0001) and onto Pd and Ag deposited on α-Al_2O_3(0001) it was found that adsorption is preferred on the metal and not on the surface site adjacent to the metal.[58] This was not due to the larger adsorption energy of CO on Ag deposited on α-Al_2O_3(0001) (E_a CO on Ag/α-Al_2O_3(0001) = 0.6 eV and E_a CO on α-Al_2O_3(0001) = 0.53 eV) but mainly because of the structural effects. Similar observations related to energy differences were found for Au/Al_2O_3 although with subtle differences.[59] CO preferentially adsorbs onto Au/α-Al_2O_3(0001) but may adsorb onto Al sites in the case of Au/Al_2O_3 (clusters – amorphous).

Table 5 Comparison of the interlayer distance in Å of different CO coverage at the partially (25%) hydroxylated surface of α-Al_2O_3(0001)

Interlayer spacing (Å)	Coverage H_2O/CO (%)	Al_{1S}	Al_{2S} OH	Al_{3S}	Al_{S4}[b]
Al_1/O_2	25/0	0.112	**0.742**	0.125	−0.211
Al_1/O_2	25/25	0.093	**0.748**	*0.364*	−0.342
Al_1/O_2	25/50	*0.321*	**0.721**	*0.324*	−0.377
Al_1/O_2	25/75	*0.280*	**0.706**	*0.290*	0.238
O_S/O_2[a]	25/0	0	**0.100**	0	0
O_S/O_2[a]	25/25	0	**0.095**	0	0
O_S/O_2[a]	25/50	0	**0.087**	0	0
O_S/O_2[a]	25/75	0	**0.084**	0	0

The subscript number indicates the layer number starting from the surface. The bold and italic numbers represent the lateral movement induced by OH and CO adsorption respectively. Interlayer distances were computed by averaging over all atoms within one layer. In the case of the O_S–H adsorption site the averaging was done with respect to the none protonated O_S counterparts. [a] The relaxation of the protonated O being a nearest neighbour of the indicated Al adsorption site is given. [b] The Al_{4S} position finds itself in 1–4 configuration with respect to adsorbed water.

Table 6 Structural and vibrational properties of CO adsorbed onto the (2 × 2) surface of Al_2O_3(0001) exhibiting a water coverage of 25%, 50%, and 75%

	(2 × 2)	(2 × 2)[b,c]	(2 × 2)[b]	(2 × 2)[b,d]	(2 × 2)[b,c]
H_2O coverage [%]	25	50	50	75	75
CO coverage [%]	25	25	25	25	25
Total coverage	50	75	75	100	100
r_{C-O} [Å]	1.148	1.147	1.147	1.147	1.147
r_{Al-C} [Å]	2.161	2.170	2.170	2.177	2.177
r_{Al-OH} [Å]	1.731	1.731	1.729	1.728[a]	1.732
r_{O-H} [Å]	0.971	0.972	0.972	0.972[a]	0.973
r_{Os-H} [Å]	0.985	0.983	0.985	0.984[a]	0.982
ν_{C-O} [cm^{-1}]	2225	2240	2240	2242	2242
Δ_{C-O} [cm^{-1}]	55	70	70	72	72
ν_{O-H} [cm^{-1}]	3936	3914	3910	3921	3914
ν_{Os-H} [cm^{-1}]	3696	3733	3710	3701	3747
CO adsorbtion energy [eV]	0.57	0.52	0.52	0.48	0.48

[a] An average value of the two equivalent H_2O molecules is presented. [b] The CO molecule is finding itself in 1–4 configuration, with respect to one adsorbed water molecule. [c] Al–OH adsorption site inflicting 1–4 position upon CO adsorption is presented. [d] Al–OH adsorption site in 1–4 position is presented.

Table 7 Comparison of the interlayer distance in Å caused by CO adsorption onto the (2 × 2) surface of α-Al_2O_3(0001) exhibiting a water coverage of 25%, 50% and 75%

Interlayer spacing [Å]	Coverage H_2O/CO[%]	Al_{1S}[b]	Al_{2S}[b]	Al_{3S}[b]CO	Al_{4S}[b] Free
Al_1/O_2	25/25	0.093	**0.748**	*0.364*	−0.342 (1–4)
Al_1/O_2	50/25	**0.737**	**0.732**	*0.312* (1–4)	−0.337 (1–4)
Al_1/O_2	75/25	**0.681**[c] (1–4)	**0.712**	*0.295* (1–4)	—
O_S/O_2[a]	25/25	0	0.094[d]	*0*	0
O_S/O_2[a]	50/25	0.107[e]	0.091[d]	*0*	0
O_S/O_2[a]	75/25	0.118[c,e]	0.089[d]	*0*	—

The subscript number indicates the layer number starting from the surface. The bold and italic numbers represent the lateral movement induced by OH and CO adsorption respectively. Interlayer distances were computed by averaging over all atoms within one layer. In the case of the O_S–H adsorption site the averaging was done with respect to the none protonated O_S counterparts. The adsorption sites finding themselves in 1–4 configuration are labelled 1–4. [a] The relaxation of the protonated O being a nearest neighbour of the indicated Al adsorption site is given. [b] The Al adsorption sites presented are being arranged in a way which allows for better comparison of interlayer changes. The subscript numbers are used to distinguish between the different adsorption sites with respect to each other, which is different from the assignment used previously. [c] An average value of the water dissociation on the Al adsorption sites in 1–4 position is presented. [d] The O_S binding to the H inflicting 1–4 configuration to the CO adsorption sites is presented. [e] O_S being next to an Al in 1–4 arrangement.

4. Conclusions

We have investigated the coverage-dependent 1–2 dissociative adsorption of water onto the (0001) surface of Al_2O_3 to study the coverage-dependent CO adsorption. Hydroxylation of the clean surface takes place *via* adsorption of the OH group on top of the Al adsorption site, while the H binds to one of the three nearest

O neighbours. An adsorption site in 1–4 configuration is characterised by its position across a six-fold ring with respect to the H of water binding to a surface O next to the Al–OH adsorption site. This arrangement causes the Al site to relax deep into the surface, therefore, being less available for further adsorption. This was verified by the fact that any adsorption taking place at this site is found to be less stable. Therefore, we concluded the most stable surfaces to be those which inflict 1–4 configuration only onto a free adsorption site. The surface exhibiting a surface hydroxylation of 75% is reported to be the most stable one.

CO adsorption onto the hydroxylated surface shows a rather complex adsorption behaviour. CO adsorption was studied with respect to increasing coverage upon a pre-hydroxylated surface. The most stable CO adsorption is found on a surface exhibiting a hydroxylation of 25% at a CO coverage of 25%, which resulted in a stronger CO adsorption energy compared to the same coverage on the clean surface. With increasing CO coverage, decreasing CO adsorption energy coupled with a decrease in the CO vibrational frequency was noted. CO adsorption onto surfaces exhibiting a hydroxylation of 25%, 50% and 75% was found to be stable, with the exception of the surface exhibiting the most stable hydroxylation (75%). An increase in surface hydroxylation also resulted in a reduced CO adsorption energy. However, an increase in the CO wavenumber was noted for surface hydroxylation at and above 50%.

References

1 V. E. Henrich and P. A. Cox, *The Surface Science of Metal Oxides*, Cambridge University Press, New York, 1994.
2 F. Pompeo, D. Gazzoli and N. N. Nichio, *Mater. Lett.*, 2009, **63**, 477.
3 M. S. Moreno, F. Wang, M. Malac, T. Kasama, C. E. Gigola, I. Costilla and M. D. Sánchez, *J. Appl. Phys.*, 2009, **105**, 083531.
4 J. Ahn and J. W. Rabalais, *Surf. Sci.*, 1997, **388**, 121.
5 J. Toofan and P. R. Watson, *Surf. Sci.*, 1998, **401**, 162.
6 I. Manassidis and M. J. Gillan, *J. Am. Ceram. Soc.*, 1994, **77**, 335.
7 M. Gautier-Soyer, F. Jollet and C. Noguera, *Surf. Sci.*, 1996, **352**, 755.
8 Z. Łodziana and J. K. Nørskov, *J. Chem. Phys.*, 2001, **115**, 11261.
9 T. Worren, K. Højrup Hansen, E. Lægsgaard, F. Besenbacher and I. Stensgaard, *Surf. Sci.*, 2001, **477**, 8.
10 J. R. B. Gomes, Z. Lodziana and F. Illas, *J. Phys. Chem. B*, 2003, **107**, 6411.
11 C. Zhou, J. Wu, T. J. D. Kumar, N. Balakrishnan, R. C. Forrey and H. Cheng, *J. Phys. Chem. C*, 2007, **111**, 13786.
12 J. A. Keller, N. Chengyu, K. Shepherd, D. R. Jennison and A. Bogicevic, *Surf. Sci.*, 2000, **446**, 76.
13 C. Niu, K. Shepherd, D. Martini, J. Tong, J. A. Kelber, D. R. Jennison and A. Bogicevic, *Surf. Sci.*, 2000, **465**, 163.
14 S. Alavi, D. C. Sorescu and D. L. Thompson, *J. Phys. Chem. B*, 2003, **107**, 186.
15 J. W. Elam, C. E. Nelson, M. A. Tolbert and S. M. George, *Surf. Sci.*, 2000, **450**, 64.
16 S. D. Chakarova-Käck, Ø. Borck, E. Schröder and B. I. Lundqvist, *Phys. Rev. B: Condens. Matter Mater. Phys.*, 2006, **74**, 155402.
17 D. C. Sorescu, J. A. Boatz and D. L. Thompson, *J. Phys. Chem. B*, 2005, **109**, 1451.
18 V. A. Ranea, W. F. Schneider and I. Carmichael, *Surf. Sci.*, 2008, **602**, 268.
19 J. M. McHale, A. Auroux, A. J. Perrotta and A. Navrotsky, *Science*, 1997, **277**, 788.
20 J. W. Elam, C. E. Nelson, M. A. Cameron, M. A. Tolbert and S. M. George, *J. Phys. Chem. B*, 1998, **102**, 7008.
21 V. Shapovalov and T. N. Truong, *J. Phys. Chem. B*, 2000, **104**, 9859.
22 K. C. Hass, W. F. Schneider, A. Curioni and W. Andreoni, *J. Phys. Chem. B*, 2000, **104**, 5527.
23 V. A. Ranea, I. Carmichael and W. F. Schneider, *J. Phys. Chem. C*, 2009, **113**, 2149.
24 A. C. Thomas and H. H. Richardson, *J. Phys. Chem. C*, 2008, **112**, 20033.
25 M. Casarin, C. Maccato and A. Vittadini, *Inorg. Chem.*, 2000, **39**, 5232.
26 C. Rohmann, J. B. Metson and H. Idriss, *Surf. Sci.*, 2011, **605**, 1694.
27 A. Soon, T. Söhnel and H. Idriss, *Surf. Sci.*, 2005, **579**, 131.
28 G. Pacchioni, G. Cogliandro and P. S. Bagus, *Surf. Sci.*, 1991, **255**, 344.
29 C. Müller, C. Freysoldt, M. Baudin and K. Hermansson, *Chem. Phys.*, 2005, **318**, 180.
30 G. Pacchioni, A. M. Ferrari and P. S. Bagus, *Surf. Sci.*, 1996, **350**, 159.
31 M. Kunat, F. Traeger, D. Silber, H. Qiu, Y. Wang, A. C. van Veen, C. Wöll, P. Kowalski, B. Meyer, C. Hättig and D. Marx, *J. Chem. Phys.*, 2009, **130**, 144703.
32 C. Rohmann, Y. Wang, M. Muhler, J. Metson, H. Idriss and C. Wöll, *Chem. Phys. Lett.*, 2008, **460**, 10.
33 A. Zecchina, D. Scarano, S. Bordiga, G. Spoto and C. Lamberti, *Adv. Catal.*, 2001, **46**, 265.
34 K. Hadjiivanov, J. Lamotte and J.-C. Lavalley, *Langmuir*, 1997, **13**, 3374.
35 L. Ferretto and A. Glisenti, *Chem. Mater.*, 2003, **15**, 1181.
36 H. Idriss, *Platinum. Met. Rev.*, 2004, **48**, 105.
37 B. E. Hayden and A. M. Bradshaw, *Surf. Sci.*, 1983, **125**, 787.
38 G. L. Griffin and J. T. Yates Jr., *J. Chem. Phys.*, 1982, **77**, 3751.
39 A. Zecchina, E. E. Platero and O. C. Areán, *J. Catal.*, 1987, **107**, 244.
40 T. H. Ballinger and J. T. Yates Jr., *Langmuir*, 1991, **13**, 3041.
41 E. N. Gribov, O. Zavorotynska, G. Agostini, J. G. Vitillo, G. Ricchiardi, G. Spoto and A. Zecchina, *Phys. Chem. Chem. Phys.*, 2010, **12**, 6474.
42 S. J. Clark, M. D. Segall, C. J. Pickard, P. J. Hasnip, M. J. Probert, K. Refson and M. C. Payne, *Z. Kristallogr.*, 2005, **220**, 567.
43 J. P. Perdew, K. Burke and M. Ernzerhof, *Phys. Rev. Lett.*, 1996, **77**, 3865.
44 H. J. Monkhorst and J. D. Pack, *Phys. Rev. B: Solid State*, 1976, **13**, 5188.

45 K. Laasonen, A. Pasquarello, R. Car, C. Lee and D. Vanderbilt, *Phys. Rev. B: Condens. Matter Mater. Phys.*, 1993, **47**, 10142.
46 B. G. Pfrommer, M. Côté, S. G. Louie and M. L. Cohen, *J. Comput. Phys.*, 1997, **131**, 233.
47 B. Hinnemann and E. A. Carter, *J. Phys. Chem. C*, 2007, **111**, 7105.
48 L. Ouyang and W.-Y. Ching, *J. Am. Ceram. Soc.*, 2001, **84**, 801.
49 J. L. Dunham, *Phys. Rev.*, 1932, **41**, 721.
50 C. G. Elles, C. A. Rivera, Y. Zhang, P. A. Pieniazek and S. E. Bradforth, *J. Chem. Phys.*, 2009, **130**, 084501.
51 A. R. Hoy and P. R. Bunker, *J. Mol. Spectrosc.*, 1979, **74**, 1.
52 C. Verdozzi, D. R. Jennison, P. A. Schultz and M. P. Sears, *Phys. Rev. Lett.*, 1999, **82**, 799.
53 J. Carrasco, J. R. B. Gomes and F. Illas, *Phys. Rev. B: Condens. Matter Mater. Phys.*, 2004, **69**, 064116.
54 Ø. Borck and E. Schröder, *J. Phys.: Condens. Matter*, 2006, **18**, 1.
55 H. A. Al-Abadleh and V. H. Grassian, *Langmuir*, 2003, **19**, 341.
56 L. Zhang, C. Tian, G. A. Waychunas and R. Y. Shen, *J. Am. Chem. Soc.*, 2008, **130**, 7686.
57 J. Scaranto and S. Giorgianni, *Mol. Phys.*, 2009, **107**, 1997.
58 J. Blomqvist, L. Lehmany and P. Salo, *Phys. Status Solidi B*, 2012, **249**, 1046.
59 E. M. Fernández and L. C. Balbás, *J. Phys. Chem. B*, 2006, **110**, 10449.
60 E. M. Fernández, R. I. Eglitis, G. Borstel and L. C. Balbás, *Comput. Mater. Sci.*, 2007, **39**, 587.